Published in final edited form as:
Ann N Y Acad Sci. 2011 September ; 1233: 41–47. doi:10.1111/j.1749-6632.2011.06166.x.

Circuit dynamics of the superior colliculus revealed by *in vitro* voltage imaging

Corinne R. Vokoun[1], **Meyer B. Jackson**[2], and **Michele A. Basso**[2,3]

[1]Molecular and Cellular Pharmacology Training Program, School of Medicine and Public Health, University of Wisconsin–Madison, Madison, Wisconsin

[2]Department of Neuroscience, School of Medicine and Public Health, University of Wisconsin–Madison, Madison, Wisconsin

[3]Department of Ophthalmology and Visual Sciences, School of Medicine and Public Health, University of Wisconsin–Madison, Madison, Wisconsin

Abstract

The superior colliculus (SC) is well known for its involvement in the conversion of sensory stimuli into motor commands. This sensorimotor integration is made possible by the collective activity of multiple neuronal connections throughout the SC. Still, the majority of SC research focuses on *in vivo* extracellular recordings of behaving monkeys or *in vitro* patch-clamp recordings from lower mammals. Here, we discuss the results of an *in vitro* voltage imaging technique in which population activity across the rodent SC circuitry was visualized to bridge the gap between single-cell recordings and whole-animal behavior.[1] The high temporal and spatial resolution of the voltage imaging technique allowed us to visualize of patterns of activity following stimulation at discrete laminae. Stimulation within either the superficial or intermediate layer showed recruitment of disparate SC circuitry. These results provide insight into the circuit dynamics and neuronal populations that underlie behavior.

Keywords

circuits; electrical stimulation; sensorimotor; eye movements

Introduction

The superior colliculus (SC) is one of several brain structures involved in sensorimotor integration. The SC is generally divided into superficial, sensory layer, and an intermediate motor layer. The SC is particularly well known for its role in processing saccadic eye movements in response to visual cues. The bulk of previous SC research has been *in vivo*, employing behavioral, electrophysiological, and computational methods in both human and non-human primates. Although powerful, these techniques cannot determine essential information about the intrinsic properties of neuronal circuits involved in behavior, nor can they directly measure neuronal activity from entire populations simultaneously. To address these limitations, new experimental techniques using *in vitro* slices of rodent brain tissue are revealing local circuit properties of the SC.

Correspondence: Michele A. Basso, University of Wisconsin, Department of Neuroscience, 1300 University Ave., Room 127 SMI Building, Madison, WI 53706, mabasso@wisc.edu.

Several recent *in vitro* investigations focused on whole-cell patch-clamp recordings made from 300–400 μm slices of rodent SC.[2] These studies show that synaptic circuitry is preserved in the slice preparation and have revealed portions of the local circuitry that were previously implied based on work *in vivo*. For example, electrophysiological and behavioral studies *in vivo* provide evidence that the superficial layers of the SC contain a map of visual space[3,4] and that the intermediate layers contain a similarly organized map of saccadic eye movement space.[5] Since the visual and movement maps are aligned,[6–8] it was predicted that sensory neurons of the superficial layers send excitatory projections to pre-motor neurons of the intermediate layers. Compelling demonstration of this excitatory pathway appeared with the application of *in vivo* anatomical and *in vitro* electrophysiological and pharmacological techniques.[2,9–11]

A downside of the whole-cell patch-clamp technique is that it is limited to single cells, and individual neurons are inadequate to account for complex behaviors. For this reason, we are using a voltage imaging technique to investigate population activity of entire neuronal circuits within the rodent SC slice.[1] This method records population membrane potentials with high temporal and spatial resolution, thereby offering a unique opportunity to bridge the gap between *in vivo* studies and single-cell recordings *in vitro*.

General methods

Male Sprague Dawley rats were rendered unconscious by CO_2 inhalation and decapitated as recommended by the Panel on Euthanasia of the Veterinary Medical Association and in accordance with the United States Public Health Service policy on the humane care and use of laboratory animals. Animal protocols were approved by the School of Medicine and Public Health Animal Care and Use Committee of the University of Wisconsin–Madison. The brains were quickly removed and sectioned in chilled artificial cerebral spinal fluid bubbled with 95% O_2 and 5% CO_2. Slices were allowed to equilibrate and were stained with the voltage-sensitive absorbance dye, RH482. The stained slices were transferred to a submerged recording chamber superfused with bubbled artificial cerebral spinal fluid on an upright microscope illuminated from below. Slices were stimulated electrically or pharmacologically, and optical signals were recorded by a 464 channel fiber-optic photodiode system.[12] At 10X magnification, the center-to-center distance of the fields of neighboring photodiodes is ~67μm. Stimulation alters the membrane potential of cells, resulting in a shift of the absorbance spectrum of RH482 and an increase in the amount of light transmitted. Recorded optical signals are a direct result of the summation of membrane potentials from the population of neurons within the photodiode area. Drugs were applied to the bath by exchange of solution. Electrical stimulation was applied as 100 μA for 200 μs. This stimulation amplitude/duration was selected to activate large neuronal circuits and is comparable to stimulus intensities from previous *in vitro* studies within the SC.[9,10,13,14] See Vokoun *et al.*[1] for detailed methods.

Results

Electrical stimulation of SC slices evoked characteristic two-component optical responses that can be visualized in individual photodiodes (Fig. 1A and 1B) as well as three-dimensional color maps (Fig. 3A and 3C; see below for further detail). These two components appeared with stimulation in both superficial and deeper layers with the amplitudes of both components varying as the stimulation site moved ventrally. The “initial-spike” is characterized by a short latency and brief duration as well as high signal amplitude. The “after-depolarization” follows the initial-spike, and is characterized by a longer latency, smaller signal amplitude and prolonged duration. Quantitatively, the initial-spike was measured from 0–10 ms after stimulation and the after-depolarization was measured from

20–160 ms after stimulation. Timing and pharmacological tests, as well as preliminary results with glutamate stimulation, indicate that both the initial-spike and the after-depolarization are dependent on synaptic signaling. Moreover, the initial-spike and after-depolarization remained unchanged in the presence of glial glutamate transporter blockers, indicating a neuronal origin for both components.

Local field potentials (LFP) were simultaneously recorded to measure extracellular fields generated by membrane currents (Fig. 1C and 1D). LFP recordings exhibited prominent initial-spikes but showed modest after-depolarizations. The observed difference in after-depolarization between voltage imaging signals of single photodiodes and LFP recordings indicates that the membrane depolarizations that comprise the after-depolarization component are likely generated by small membrane currents. On the other hand, the large membrane depolarizations that make up the initial-spike component are generated by large synchronous membrane currents. Voltage imaging of the fish optic tectum (SC homolog) showed similar results.[15]

In addition to analyzing the response of single photodiodes, we examined the spatial patterns of population responses within the SC. Due to its higher signal amplitude, the initial-spike component will be used here to exemplify signal spread throughout the tissue (Fig. 2). For a more in-depth analysis of both signal components, see Vokoun *et al.*[1]. Spatial response maps with signal encoded as color (smoothed by linear interpolation and Gaussian spatial filtering) were created to illustrate the response of the SC to superficial layer (SGS) and intermediate layer (SGI) stimulation. The color scale of each response map was normalized to its own minimum (dark blue) and maximum (red). Following a single pulse of electrical stimulation (100 μA, 200 μs) to the SGS, optical signals spread ~500 μm medially and laterally (intralaminarly) from the site of stimulation and interlaminarly ~800 μm. The response was maximal at the site of stimulation and radiated mediolaterally and ventrally over time (Fig. 2A). Due to normalization, the high-amplitude signals within the superficial layer obscure lower-amplitude signals within the intermediate layer. For clarity, a plot was created to show dorsoventral signal spread over time, with signal amplitude encoded as color (Fig. 3A). As mentioned above, the greatest amplitude of both temporal components exists within the superficial layer and spreads ventrally over time. When the color scale is renormalized to exclude the high-intensity signals of the superficial layers, it is easier to see the optical signals within the upper and lower SGI. The signals in the SGI remain above baseline for at least 80 ms (Fig. 3A, inset). Moreover, photodiodes selected from each of the layers show the relative intensities of signal within the laminae (Fig. 3B). A further analysis of the latency of signal spread within and between layers can be found in Vokoun *et al.*[1] Interlaminar spread into the intermediate and deep layers is in agreement with previous patch-clamp results that describe a ventrally directed excitatory pathway.[9,10]

Single-pulse stimulation of the SGI resulted in a different pattern of signal spread (Fig. 2B). Membrane depolarization was minimal at the site of stimulation and did not spread throughout the layer. However, SGI stimulation did result in interlaminar signal propagation into the superficial layers, where it then spread widely throughout the SGS (~600 μm medially and laterally from the site of stimulation). In fact, when Gaussian functions were fitted to the mediolateral signals throughout SGS, SGI stimulation produced a wider distribution than did SGS stimulation (Fig. 2C). Thus, intralaminar signals spread further throughout the SGS even though stimulation occurred in the SGI. Additionally, the maximum amplitude following SGI stimulation occurred at the border between the SGS and the optic layer (SO), a location slightly more ventral than that observed after SGS stimulation. The fact that SGI stimulation elicited excitatory responses in the SGS and SO suggests the existence of a dorsally directed excitatory pathway from SGI to SGS. Additional evidence of this interlaminar pathway is shown in Figure 3C and 3D. A plot of

dorsoventral activity shows little activation of the intermediate layer following stimulation (Fig. 3C). Individual photodiodes from each of the laminae show the majority of the signal travels dorsally into the superficial layers over time (Fig. 3D). Preliminary results using pharmacological stimulation of the SGI with glutamate show similar patterns of activation within the SGS, indicating that the electrically evoked superficial layer responses were not a result of antidromic activation of descending axons. The distinctly different patterns of signal spread elicited by SGS and SGI stimulation imply that disparate local circuits are activated with each stimulation site.

Further pharmacological tests were performed to evaluate the role of various receptor types on the response patterns within the SC following both SGS and SGI stimulation. First, we tested the contribution of AMPA and NMDA receptors on synaptic signaling. Although NMDA receptor antagonists alone (APV, 50 μM) had little effect on the signals, the AMPA receptor antagonist NBQX (5 μM) greatly reduced the amplitude of both temporal components, indicating a strong synaptic contribution to the voltage imaging signals. The reduction in signal was especially clear in superficial layers, which show the highest response amplitudes for both sites of stimulation. In other words, NBQX reduced both the intralaminar and interlaminar signal spread, independent of the site of stimulation. This is further evidence for the activation of a ventrally directed synaptic pathway with superficial layer stimulation and activation of a dorsally directed synaptic pathway with intermediate layer stimulation. Subsequent application of tetrodotoxin (300 nM) in the continued presence of NBQX blocked the remaining signal, demonstrating that residual responses after NBQX addition were due to voltage-gated Na^+ channels.

We also tested the action of $GABA_A$ receptor antagonists bicuculline (50 μM) and gabazine (SR95531, 5 μM), because the SC is known to be influenced by local $GABA_A$ inhibition as well as remote tonic inhibition via substantia nigra pars reticulata.[2,13,16–21] For stimulation in either SGS or SGI, $GABA_A$ receptor antagonists generally increased the amplitude of voltage imaging signals, with the greatest effect (approximate two-fold increase) on the after-depolarization component. In addition, $GABA_A$ receptor blockade increased the mediolateral and dorsoventral spread of signal following both SGS and SGI stimulation. These results indicate a strong and widespread role for $GABA_A$ receptors within the circuitry of the SC.

Discussion

Here, we reviewed the results of *in vitro* voltage imaging experiments largely from Vokoun *et al.*,[1] in which the voltage-sensitive absorbance dye, RH482, was used to image evoked responses throughout coronal slices of rodent SC. This technique is sensitive enough to respond with microsecond kinetics, and yet the scope is still broad enough to view population activity of entire neuronal circuits. This technique therefore offers the opportunity to answer questions about complex neuronal circuits that other techniques cannot.

We found that single-pulse electrical stimulation of the SC elicited a characteristic two-component response. The first component, the initial-spike, rose and fell within 10 ms. This may result from the activation of narrow-field and wide-field vertical neurons, both of which can produce single action potentials followed by slow depolarizations in response to SGS stimulation.[22] The second component, the after-depolarization, arose after the initial-spike and lasted more than 100 ms. This component may be the product of prolonged asynchronous bursting, which can be produced by narrow-field, wide-field, and horizontal neurons. It is also possible that the after-depolarization reflects recurrent activation via collaterals arising from premotor cells[23–26] or activity of intrinsic voltage-gated channels.

Regardless of the neuronal underpinning of either component, pharmacological studies demonstrated that signals represent the sum of hyperpolarizing and depolarizing potentials from populations of neurons.

Following SGS stimulation, intralaminar responses extended ~500 μm medially and laterally from the site of stimulation, and interlaminar responses spread ~800 μm into the intermediate and deep layers. In contrast, SGI stimulation elicited a restricted pattern of activity within the layer of stimulation. However, the signals spread dorsally into the SGS, where they then spread ~600 μm medially and laterally from the site of stimulation. The high-amplitude intralaminar signal observed within the superficial layers following stimulation at either lamina most likely results from the activation of the wide dendritic trees of horizontal and wide-field vertical cells. Superficial stimulation of these cell types would funnel the activity of large dendritic trees into smaller axonal projections, resulting in the lower population activity seen in the intermediate layer. Together, these results indicate that single-pulse electrical stimulation is sufficient to influence a large region of the SC, both within and between layers. Pharmacological tests support the hypothesis that these signals are largely driven by AMPA-type glutamatergic receptor activation and constrained by $GABA_A$ receptor–mediated inhibition. These results agree with previous findings that indicate the existence of functional linkages between the layers of the SC.[9–11,23,27]

A further point of interest is that SGS and SGI stimulation elicited distinct spatial patterns of signal spread. This dissimilarity provides compelling evidence that different subpopulations of neurons making up the SC circuitry are activated upon stimulation in different SC laminae. This leads us to the more novel result presented in Vokoun *et al.*[1] in support of a dorsally directed excitatory pathway from SGI to SGS. This result is important because a dorsally directed excitatory pathway has been hypothesized to exist based on extracellular recordings of sensory neurons in the SGS of monkey.[28,29] Although a dorsally directed inhibitory pathway has been studied *in vitro,*[19,30] prior anatomical and physiological studies failed to identify a dorsally directed excitatory pathway *in vitro*. The incidence of SGI neurons that send excitatory projections dorsally is likely to be lower than the incidence of SGS neurons that send excitatory projections ventrally. This would explain why a population-level technique is capable of observing such phenomena and previous patch-clamp studies could have easily overlooked this type of circuitry. Moreover, the possibility that SGS responses reflect the antidromic activation of axons from SGS neurons appears unlikely in light of our timing analyses and pharmacological experiments, which suggest that the vast majority of the signal (particularly the high-amplitude signal within the SGS) is synaptically driven. Furthermore, preliminary experiments using focal application of glutamate to stimulate the tissue without activated axonal fibers reveal patterns of activity virtually identical to those evoked by electrical stimulation.

The primary motive for performing *in vitro* experiments such as these is to understand neuronal circuits that underlie complex behaviors studied *in vivo* as well as to bridge a gap between *in vitro* patch-clamp results and *in vivo* electrophysiological results. Moreover, we would like to gain a broader understanding of the local circuitry of the SC and its role in sensorimotor integration and saccadic eye movements. Rodent SC neurons have been well characterized physiologically and anatomically, but their relationship to whole-animal behavior is unknown. By contrast, the activity of monkey SC neurons has been well characterized in relation to behavior, but their detailed cellular physiology and connectivity remain unknown. Our experiments are a first step toward bridging this gap in knowledge.

Acknowledgments

This work was supported by the Alice R. McPherson Endowment for the Visual Sciences at the University of Wisconsin Eye Research Institute (M.A.B. and M.B.J.) and by a NIH award (EY019663, M.A.B. and M.B.J.). Support also came from the Parkinson's Disease Foundation Summer Student Fellowship program (C.R.V.).

References

1. Vokoun CR, Jackson MB, Basso MA. Intralaminar and interlaminar activity within the rodent superior colliculus visualized with voltage imaging. J Neurosci. 2010; 30:10667–10682. [PubMed: 20702698]
2. Isa T, Hall WC. Exploring the superior colliculus *in vitro*. J Neurophysiol. 2009; 102:2581–2593. [PubMed: 19710376]
3. Lane RH, Allman JM, Kaas JH. Representation of the visual field in the superior colliculus of the grey squirrel (Sciurus carolinensis) and the tree shrew (Tupaia glis). Brain Res. 1971; 26:277–292. [PubMed: 5547178]
4. Cynader M, Berman N. Receptive-field organization of monkey superior colliculus. J Neurophysiol. 1972; 35:187–201. [PubMed: 4623918]
5. Robinson DA. Eye movements evoked by collicular stimulation in the alert monkey. Vis Res. 1972; 12:1795–1808. [PubMed: 4627952]
6. Schiller PH, Stryker M. Single-unit recording and stimulation in superior colliculus of the alert rhesus monkey. J Neurophysiol. 1972; 35:915–924. [PubMed: 4631839]
7. Goldberg ME, Wurtz RH. Activity of superior colliculus in behaving monkey: I. Visual receptive fields of single neurons. Journal of Neurophysiology. 1972; 35:542–559. [PubMed: 4624739]
8. Wurtz RH, Goldberg ME. Activity of superior colliculus in behaving monkey: III. Cells discharging before eye movements. J Neurophysiol. 1972; 35:575–586. [PubMed: 4624741]
9. Lee PH, et al. Role of intrinsic synaptic circuitry in collicular sensorimotor integration. Proc Natl Acad Sci USA. 1997; 94:13299–13304. [PubMed: 9371840]
10. Isa T, Endo T, Saito Y. The visuo-motor pathway in the local circuit of the rat superior colliculus. J Neurosci. 1998; 18:8496–8504. [PubMed: 9763492]
11. Behan M, Appell PP. Intrinsic circuitry in the cat superior colliculus: projections from the superficial layers. J Comp Neurol. 1992; 315:230–243. [PubMed: 1372013]
12. Wu, JY.; Cohen, LB. Fast multisite optical measurements of membrane potential. In: Mason, WT., editor. Fluorescent and luminescent probes for biological activity. Academic; London: 1993. p. 389-404.
13. Lee PH, Schmidt M, Hall WC. Excitatory and inhibitory circuitry in the superficial gray layer of the superior colliculus. J Neurosci. 2001; 21:8145–8153. [PubMed: 11588187]
14. Phongphanphanee P, Kaneda K, Isa T. Spatiotemporal profiles of field potentials in mouse superior colliculus analyzed by multichannel recording. J Neurosci. 2008; 28:9309–9318. [PubMed: 18784311]
15. Kinoshita M, et al. Multiple-site optical recording for characterization of functional synaptic organization of the optic tectum of rainbow trout. Eur J Neurosci. 2002; 16:868–876. [PubMed: 12372023]
16. Chevalier G, et al. Disinhibition as a basic process in the expression of striatal functions. I. The striato-nigral influence on tecto-spinal/tecto-diencephalic neurons. Brain Res. 1985; 334:215–226. [PubMed: 2859912]
17. Chevalier G, Deniau JM. Disinhibition as a basic process in the expression of striatal functions. Trends Neurosci. 1990; 13:277–280. [PubMed: 1695403]
18. Hall WC, Lee P. Interlaminar connections of the superior colliculus in the tree shrew. I. The superficial gray layer. J Comp Neurol. 1993; 332:213–223. [PubMed: 8331213]
19. Lee PH, et al. Identity of a pathway for saccadic suppression. Proc Natl Acad Sci USA. 2007; 104:6824–6827. [PubMed: 17420449]
20. Behan M, et al. Chemoarchitecture of GABAergic neurons in the ferret superior colliculus. J Comp Neurol. 2002; 452:334–359. [PubMed: 12355417]

21. Kaneda K, et al. Nigral inhibition of GABAergic neurons in mouse superior colliculus. J Neurosci. 2008; 28:11071–11078. [PubMed: 18945914]
22. Özen G, Augustine GJ, Hall WC. Contribution of the superficial layer neurons to premotor bursts in the superior colliculus. J Neurophysiol. 2000; 84:460–471. [PubMed: 10899219]
23. Mooney RD, et al. The projection from the superficial to the deep layers of the superior colliculus: an intracellular horseradish peroxidase injection study in the hamster. J Neurosci. 1988; 8:1384–1399. [PubMed: 3357022]
24. Moschovakis AK, Karabelas AB, Highstein SM. Structure-function relationships in the primate superior colliculus. I. Morphological classification of efferent neurons. J Neurophysiol. 1988; 60:232–262. [PubMed: 3404219]
25. Hall WC, Lee P. Interlaminar connections of the superior colliculus in the tree shrew. III: The optic layer. Vis Neurosci. 1997; 14:647–661. [PubMed: 9278994]
26. Pettit DL, et al. Local excitatory circuits in the intermediate gray layer of the superior colliculus. J Neurophysiol. 1999; 81:1424–1427. [PubMed: 10085368]
27. Lee PH, Hall WC. Interlaminar connections of the superior colliculus in the tree shrew. II: Projections from the superficial gray to the optic layer. Vis Neurosci. 1995; 12:573–588. [PubMed: 7544610]
28. Goldberg ME, Wurtz RH. Activity of superior colliculus in behaving monkey. II. Effect of attention on neuronal responses. J Neurophysiol. 1972; 35:560–574. [PubMed: 4624740]
29. Wurtz RH, Mohler CW. Organization of monkey superior colliculus: enhanced visual response of superficial layer cells. J Neurophysiol. 1976; 39:745–765. [PubMed: 823303]
30. Phongphanphanee P, et al. A circuit model for saccadic suppression in the superior colliculus. J Neurosci. 2011; 31:1949–1954. [PubMed: 21307233]

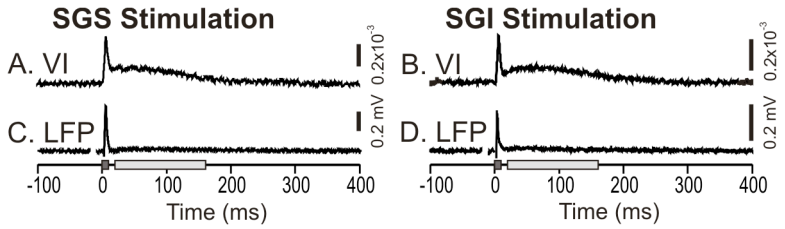

Figure 1.

Electrical stimulation evoked two component optical responses.(**A**) Voltage imaging (VI) traces following SGS stimulation (recorded within the SGS). Trace shows 100 ms prior to and 400 ms following electrical stimulation (applied at time 0). Responses are shown as ΔI/I (change in light intensity relative to resting light intensity). Initial-spike is shown by a dark gray bar on the timescale at 0–10 ms. After-depolarization is shown by a light gray bar on the timescale at 20–160 ms. A scale bar is shown to the right of the trace. (**B**) Voltage imaging trace following SGI stimulation (recorded within the SGS). Arrangement is the same as in panel A. (**C**) Local field potential (LFP) recordings following SGS stimulation. The LFP trace was recorded from approximately the same location as the voltage imaging trace was selected. (**D**) Local field potential recording following SGI stimulation. Arrangement is the same as in panel C. Modified from Vokoun *et al.*[1]

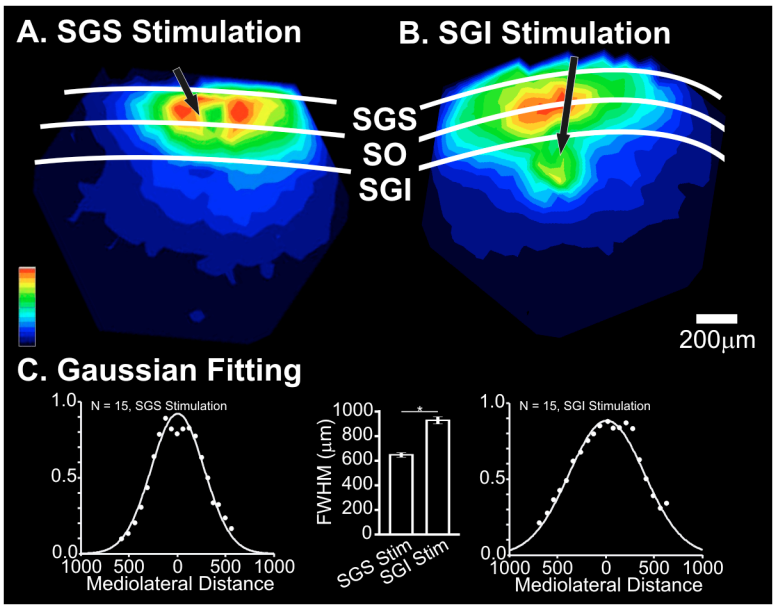

Figure 2.

(**A**) Colormap image of the initial-spike signal amplitude following superficial layer stimulation. The amplitudes were normalized to the maximum amplitude of the initial-spike component (0–10 ms) with hotter colors indicating higher signal amplitudes. White lines and labels denote laminae; stratum griseum superficiale (SGS), stratum opticum (SO), and stratum griseum intermediale (SGI). Black arrow indicates placement of the stimulating electrode. Scale bars show 200 μm. (**B**) Colormap image of the initial-spike signal amplitude following intermediate layer stimulation. (**C**) Population graph of the normalized initial-spike signal amplitude following SGS stimulation (far left panel) and SGI stimulation (far right panel). Gaussian functions (white curves) were fitted to the data points (white dots) from each experiment ($N = 15$). The mean and standard error of the full width at half maximum (FWHM) of the Gaussian distributions are shown in bar form between the two distributions. * $P < 0.05$. Modified from Vokoun *et al.*[1]

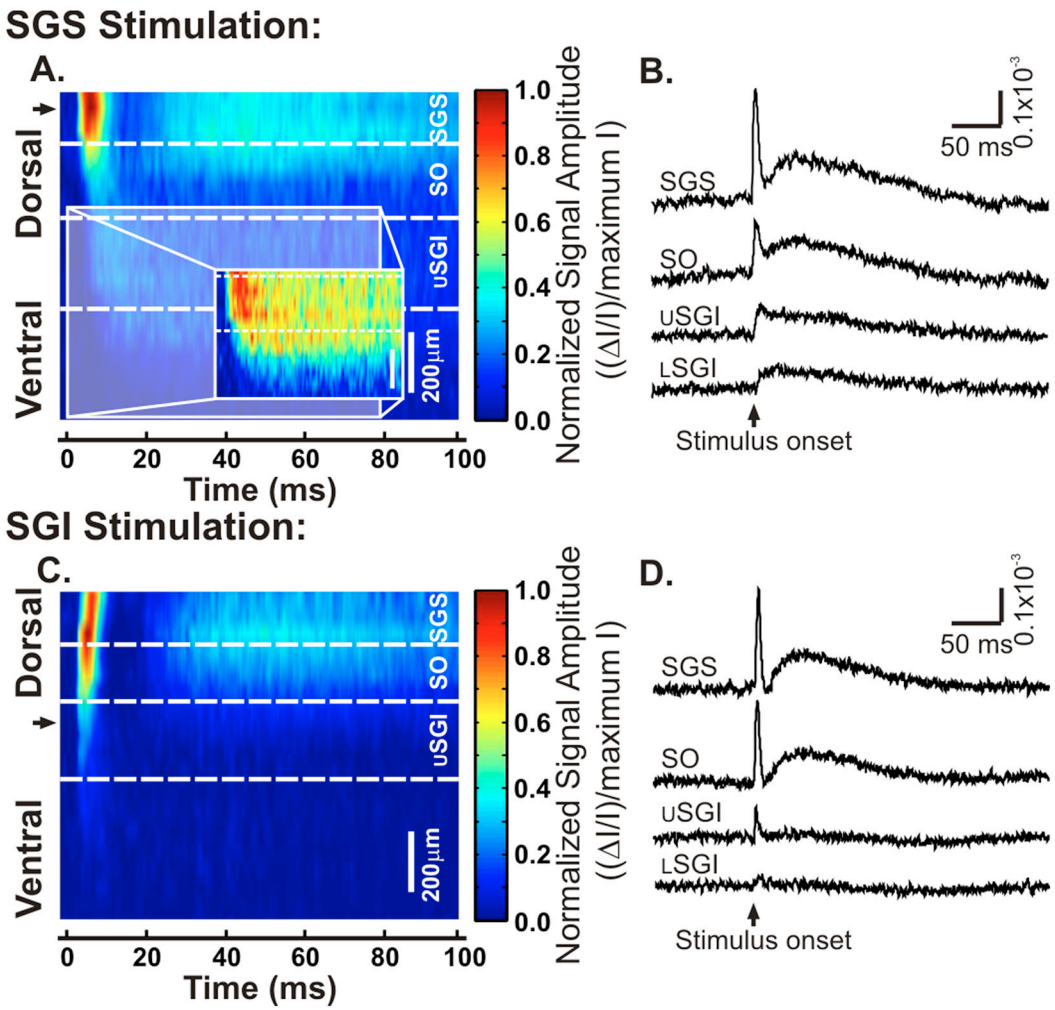

Figure 3.

(**A**) Three-dimensional color map showing the time course of response spread following electrical stimulation of the SGS. The dorsoventral location along a selected path in the SC is shown on the y-axis. A black arrow indicates the site of stimulation. The white scale bar shows 200 μm. Time is shown on the x-axis from 0–100 ms after stimulation. Signal intensity is normalized to the maximum of all diodes along the selected path. Hotter colors indicate higher signal amplitude. Dotted white lines demark approximate boundaries of the labeled laminae. $_{U}$SGI, upper SGI; $_{L}$SGI, lower SGI. Inset shows 0–80 ms renormalized to the maximum intensity within the selected dorsoventral region to show the spread of activity into the SGI. (**B**) Representative photodiode traces selected from each lamina along the dorsoventral path. The upward arrow indicates the time of stimulation. Responses are shown as ΔI/I (change in light intensity relative to resting light intensity). (**C–D**) Same as A and B, respectively, for SGI stimulation. Modified from Vokoun *et al.*[1].